IEEE Photonics Journal
An IEEE Photonics Society Publication

Open Access

Creation of an Arbitrary Electromagnetic Illusion Using a Planar Ultrathin Metasurface

Volume 9, Number 4, August 2017

Ren Wang, *Student Member, IEEE*
Bing-Zhong Wang, *Senior Member, IEEE*
Zhi-Shuang Gong
Xiao Ding, *Member, IEEE*

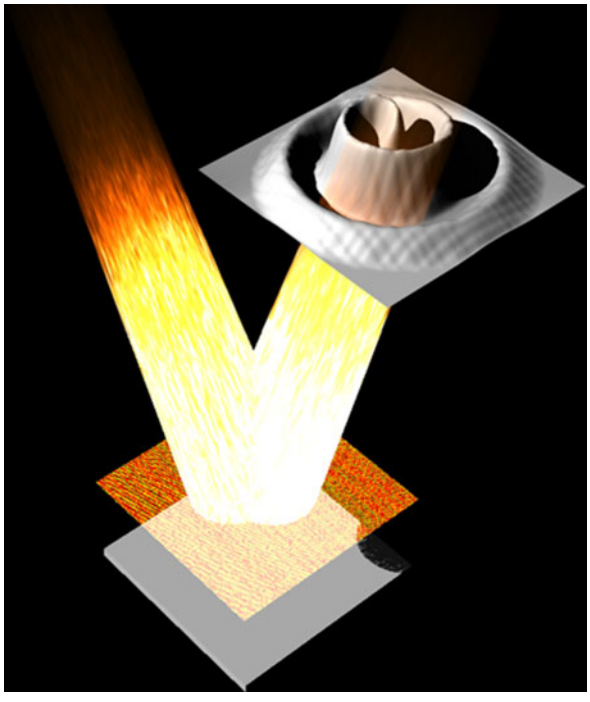

DOI: 10.1109/JPHOT.2017.2733044
1943-0655

IEEE photonics SOCIETY

IEEE

Creation of an Arbitrary Electromagnetic Illusion Using a Planar Ultrathin Metasurface

Ren Wang, *Student Member, IEEE*, Bing-Zhong Wang, *Senior Member, IEEE*, Zhi-Shuang Gong, and Xiao Ding, *Member, IEEE*

Institute of Applied Physics, University of Electronic Science and Technology of China, Chengdu 610054, China

DOI:10.1109/JPHOT.2017.2733044

Manuscript received May 24, 2017; revised July 23, 2017; accepted July 25, 2017. Date of publication July 28, 2017; date of current version August 8, 2017. This work was supported in part by the National Natural Science Foundation of China under Grants 61331007, 61361166008, and 61401065 and in part by the EHF key Laboratory of Fundamental Science under Project A03010023801171003.
Corresponding author: Ren Wang (e-mail: rwang.uestc@hotmail.com).

Abstract: An electromagnetic illusion method with planar metasurfaces is demonstrated numerically and experimentally. In the method, the scattering field of an arbitrary object can be built by using a planar ultrathin metasurface with dual-polarized subwavelength unit cells. The proposed planar illusion metasurface can disguise itself as an arbitrary object when the incident wave comes from a relative wide angle range, which means the proposed method is of great practical value.

Index Terms: Arbitrarily-sharped object, dual-polarization, electromagnetic illusion, planar ultrathin metasurface.

1. Introduction

Electromagnetic cloak is a device used to make objects invisible to waves. With the assistance of metamaterials, transformation optics becomes a powerful tool to build cloaking devices [1]–[3]. In [1], an electromagnetic cloak with metamaterials was realized at microwave frequencies based on transformation optics. Later, optical cloak was also realized [3]. Reference [4] pointed out that cloak was a special illusion device and transformation optics could be used to generate a general illusion, which can make one object seem like other objects. By inheriting this concept, some microwave and optical illusion devices were designed based on the transformation optics [5]–[7]. Similar to the method using transformation optics, scattering cancellation method can also be used for cloak and illusion devices by covering targets with a metamaterial cylinder [8]–[10]. Based on quasi–conformal mapping technique [11], carpet configuration was used to design cloak devices by rebuilding the reflected wavefront of the clock as if it were reflected from a flat surface. Carpet cloaks have been realized for microwave applications [12], [13], optical applications [14]–[17], and acoustic applications [18]. For the above methods using transformation optics and scattering cancellation, the object is protected from field by covering cloak or illusion devices. Different from these methods, the object is allowed to be exposed to field in holography method, which is based on Fourier optics [19]–[22].

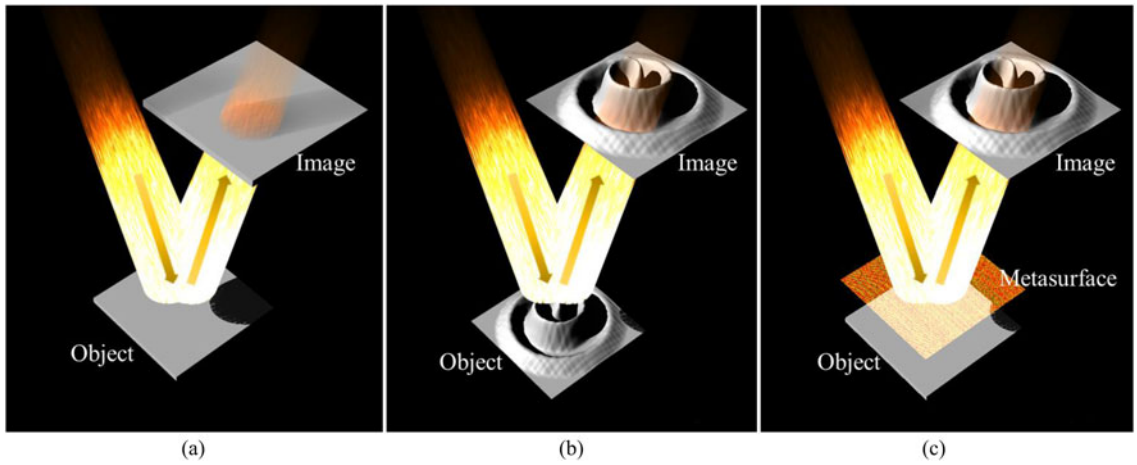

Fig. 1. Schematic diagram of creating an illusion with a planar metasurface. (a) A planar object covered with nothing. (b) An uneven object covered with nothing. (c) An object covered with designed planar metasurface. An illusion image can be observed.

Recently, the development of metasurfaces pointed out a new way to build cloak and illusion devices by directly manipulating wavefront. The metasurface with subwavelength elements can locally tailor the electromagnetic or mechanical response at subwavelength scale [23]–[28]. Based on metasurfaces, some electromagnetic carpet cloaks were proposed at microwave frequencies [29]–[31], optical frequencies [32], [33], and acoustics [34]. In [29], the desired field distribution was generated by reconstructing the fields at the metasurface in calculation to makes the reflected wavefront resemble a flat surface. In [30] and [31], the experimental demonstration of metasurface-based carpet cloaks was proposed at microwave frequencies. In [33], an ultrathin invisible skin cloak was experimentally demonstrated to conceal objects by restoring the reflected phase at optical wavelength. In 2017, a novel illusion method using planar metasurfaces was proposed in acoustics [35]. The phase distribution of the planar metasurfaces for the illusion applications was opposite to the phase distribution on cloak devices. By using this method, the flat metasurface can create the scattering field of the virtual object.

In this paper, the planar metasurface illusion method is numerically and experimentally demonstrated at microwave frequencies. Firstly, the operation principle of creating arbitrary electromagnetic illusions by using planar ultrathin metasurfaces is analyzed. Afterwards, a dual-polarized metasurface unit cell is proposed and a planar electromagnetic illusion metasurface with proposed unit cells is designed. The proposed illusion metasurface can disguise itself as an arbitrary object when the incident wave comes from a relative wide angle range, which means the proposed method is of great practical value. At last, the proposed planar illusion metasurface is fabricated and measured. The measured and simulated electric fields agree well.

2. Operating Principle of the Planar Metasurface

The schematic diagram of creating illusions with planar metasurfaces is shown in Fig. 1. To disguise a planar illusion metasurface as an arbitrary virtual object, the scattering field of the planar metasurface should look like that of the virtual object. Thus, if the scattering field of the illusion planar metasurface is used to reconstruct the scatterer with traditional imaging methods, the virtual object should be obtained. The essence of this method is to control scattering field by directly manipulating wavefront using metasurfaces. In principle, the metasurface can have arbitrary shapers for this purpose. However, the ultrathin planar metasurface, as the simplest shaper, is a good choice because it is easily-fabricated and has a low profile. For the cloaking metasurface conformed with an object, the reflected phase should have a gradient distribution $\Delta\varphi = \pi - 2k_0 z(x, y)\cos(\theta)$ to make the reflected wave seem like scattered from a flat metallic surface [29]–[34], where k_0, $z(x, y)$, and

θ are the wavenumber in free space, the shaper of the object, and the incident angle, respectively. As an opposite process, to make the reflected wave of a planar illusion metasurface seem like scattered from an arbitrary virtual object, the reflected phase of the planar illusion metasurface should have a gradient distribution $\Delta\varphi_m = \varphi_o + 2k_0 z_o(x, y)\cos(\theta)$, where $\Delta\varphi_m$, φ_o, and $z_o(x, y)$ are the phase gradient of the planar illusion metasurface, the reflected phase of the virtual object, and the shaper of the virtual object, respectively. From the equation, we can see that the virtual object $z_o(x, y)$ and the original reflected phase φ_o have no limiting conditions for operation, which indicates that this method is suitable for arbitrary structures with arbitrary materials.

3. Dual-Polarized Metasurface Units

To design a planar illusion metasurface and directly manipulate wavefront, a primary step is designing metasurface unit cells with several discrete reflected phases. Because the incident wave may have arbitrary polarizations, the metasurface should have good performances to orthogonally polarized incident waves. According to the required phase gradient equation of the planar illusion metasurface introduced in the above section, the phase gradient at a certain position is only related to the height of virtual object and incident angle instead of incident polarization, therefore, for dual-polarized applications, the responses of a metasurface unit cell should be the same to orthogonal polarized incident waves. A simple and efficient way to obtain the same response to orthogonal polarized waves is to design square metasurface cell with symmetric structures.

A dual-polarized metasurface unit cell is shown in Fig. 2. The unit cell is composed of a backed ground, dielectric substrate, and two orthogonal rectangular patches. The dielectric substrate has a relative permittivity of 4.4 and a thickness of 1.6 mm, about 0.03λ corresponding to 5.8 GHz. The side length of the square unit cell is 12.9 mm, about 0.25λ. The reflected phase can be adjusted by changing the length and width of the rectangular patch. The reflected phase map and reflected magnitude map versus different structure parameters of the proposed unit cell are shown in Fig. 2(a) and (b), respectively. With the change of patch size, the reflected phase can change within the range of $-180°\sim180°$, and the reflected magnitude is more than 0.8 in the map except two small areas. Nine reflected phases at 5.8 GHz, 180°, 140°, 100°, 60°, 20°, $-20°$, $-60°$, $-100°$, and $-140°$, are selected to build the planar illusion metasurface. For the sake of convenience, l and w are both set as the side length of the square unit cell for the 180° case, which means that the unit cell is fully covered with copper layer. For the other reflected phase, w is fixed as 6 mm, and l changes from 7.3 mm to 11.83 mm, as the light green line shows in Fig. 2. In the area that the light green line indicates, the reflected phases can cover the range from $-140°$ to 140° and the reflected amplitudes are more than 0.8. The reflected phases and reflected magnitudes corresponding to selected structure parameters are shown in Fig. 2(c) and (d), which can remain relatively stable from 5.6 GHz to 6 GHz.

4. Creation of an Arbitrary Illusion Using a Planar Metasurface

To demonstrate the performance of the proposed method that creating arbitrary electromagnetic illusions using planar metasurfaces, modified Peaks function is used to generate a metallic rugged structure. Peaks is a general test function to demonstrate three-dimensional plotting commands in Matlab, which has several peaks and valleys. The modified Peaks function used in this paper is

$$z(x, y) = \lambda/16.2\left\{3(1 - x/2\lambda)^2 e^{\left[-(x/2\lambda)^2-(y/2\lambda+1)^2\right]} - 10[x/10 - (x/2\lambda)^3 - (y/2\lambda)^5]\, e^{\left[-(x/2\lambda)^2-(y/2\lambda)^2\right]} - 1/3e^{\left[-(x/2\lambda+1)^2-(y/2\lambda)^2\right]}\right\} \quad (1)$$

where λ is the wavelength in free space corresponding to 5.8 GHz. The Peaks structure generated according to (1) is shown in Fig. 3(a). In the simulation, the Peaks structure is generated in CST Microwave Studio with Matlab program. The side lengths in X and Y directions of the pixel are both 0.25λ, which is the same as the side length of the unit cell designed in above section. The vertical

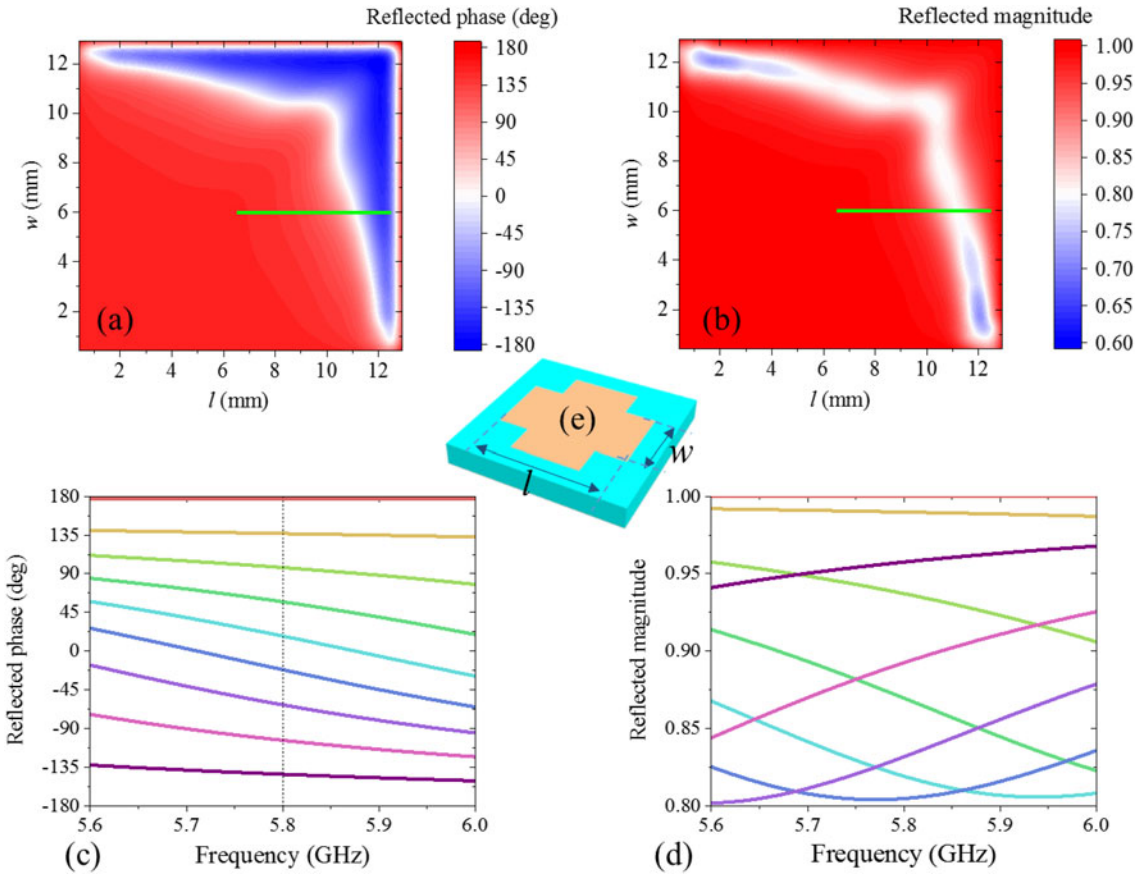

Fig. 2. Dual-polarized metasurface unit cell. (a) Reflected phase map and (b) reflected magnitude map versus different structure parameters of the proposed metasurface unit cell. The light green line indicates the position of the structure dimensions selected for illusion metasurface application. Nine groups of parameters corresponding to nine reflected phases at 5.8 GHz are selected. (c) Reflected phases and (d) reflected magnitudes corresponding to selected structure parameters. (e) Structure of the proposed dual-polarized metasurface unit, which has two orthogonal rectangular patches.

distance between the top and bottom of the Peaks structure is about λ. Here, a special scenario, i.e., the virtual object is metallic and the incident electromagnetic wave comes from the normal direction, is used to generate a planar illusion metasurface with the proposed unit cells. For this scenario, the phase gradient of the planar illusion metasurface should be

$$\Delta\varphi_m = \pi + 2k_0 z_o(x, y) \tag{2}$$

where $\Delta\varphi_m$ and $z_o(x, y)$ are the phase gradient of the planar illusion metasurface and the shaper of the virtual object, respectively. According to (2), the required phase distribution of the Peaks structure generated using (1) is shown in Fig. 3(b). The required phase changes from $-120°$ to $550°$ in the required area. A planar illusion metasurface with fully backed copper ground is generated according to Fig. 3(b) with the proposed unit cells, as shown in Fig. 3(c) and (d).

Although the proposed illusion metasurface is designed according to the required phase map for normal incidence, it can still work well in a relative wide incident angle range, as shown in Figs. 4 and 5. The incident waves for Peaks structure and its corresponding illusion metasurface are the same, which are Y-polarized plane waves with an incident angle θ. From Fig. 4, we can see that both the field of the metasurface and Peaks structure change with the incident angle and the field distributions of illusion metasurface and Peaks structure are similar even when the incident angle is 30°. The normalized scattering patterns at 5.8 GHz corresponding to different

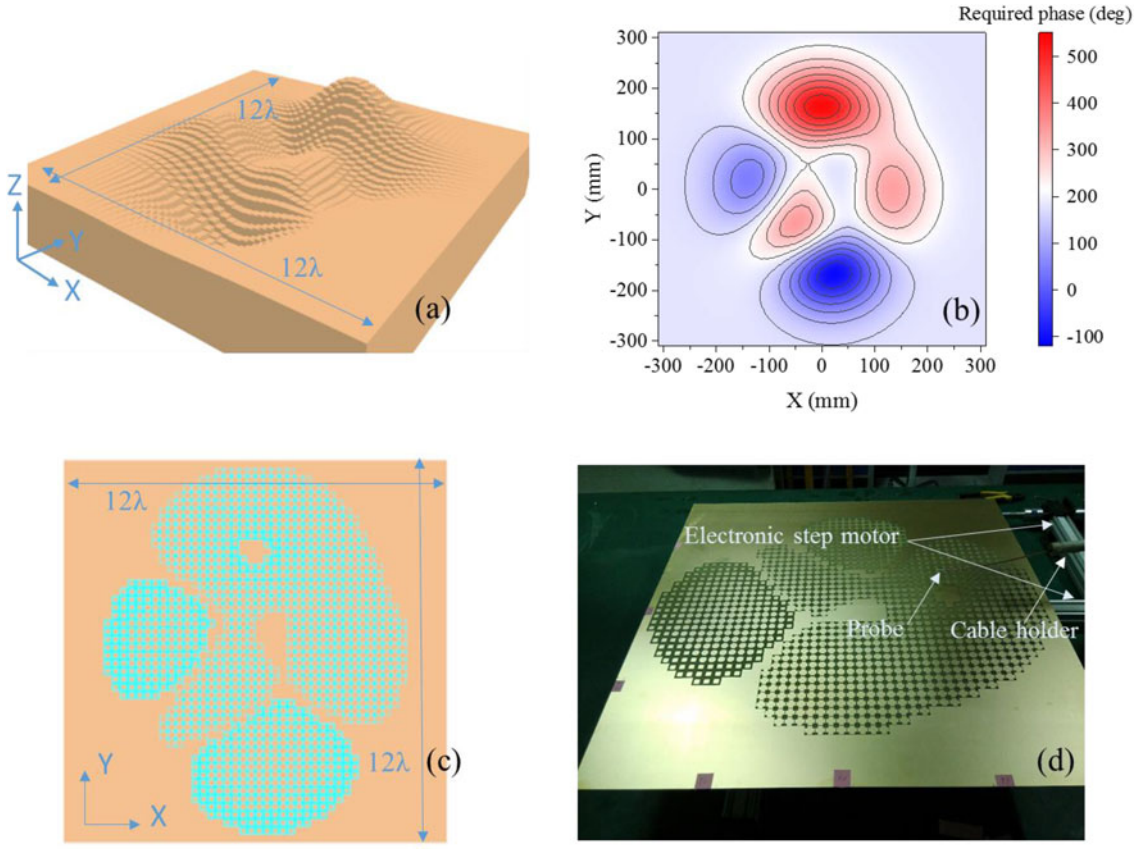

Fig. 3. Geometry of the Peaks structure and its corresponding illusion metasurface. (a) Peaks structure generated with modified Peaks function. The vertical distance between the top and bottom of the structure is about λ. (b) The required phase map for a planar illusion metasurface to disguise itself as the Peaks structure in (a) when the electromagnetic wave is normally incident. (c) A planar illusion metasurface generated according to (b) with the unit cells shown in Fig. 2. (d) Photograph of the proposed illusion metasurface in the measurement configuration. The metasurface is placed on a tray, which can be moved in a 2D plane using step motors. A probe is placed under a horn source to measure the field.

incident waves are shown in Fig. 5. Four large beams can be seen in the XZ-plane patterns of both metasurface and Peaks structure because of the complex scattering. With the increasing of incident angle, the main scattering directions of metasurface and Peaks structure increase simultaneously. The main polarized components of illusion metasurface and Peaks structure are the same in each incident case and each plane, and the scattering patterns of main polarized components of illusion metasurface and Peaks structure are similar under all the incident angles of 0°, 10°, 20°, and 30°. In addition, the main polarized component is more than 35 dB larger than the other component, which means the proposed illusion metasurface does not induce undesired cross-polarized component. From the above analysis, we can see that the scattering field of an arbitrary object can be built by a planar metasurface according to the proposed method. In other word, we can create an arbitrary electromagnetic illusion using a planar ultrathin metasurface.

From (2), we can see that the phase gradient is related to the height of the virtual object instead of the polarization of incident electromagnetic wave. For a certain position of the metasurface, the height is the same no matter what the polarization of the incident wave is, which means the metasurface's responses to orthogonally polarized incident waves only depend on the unit-cell's responses to orthogonally polarized incident waves. From the section about unit-cell design, the proposed square unit cell with symmetric structure has the same responses to orthogonal polarized incident waves. Therefore, the proposed illusion metasurface should have good performances to

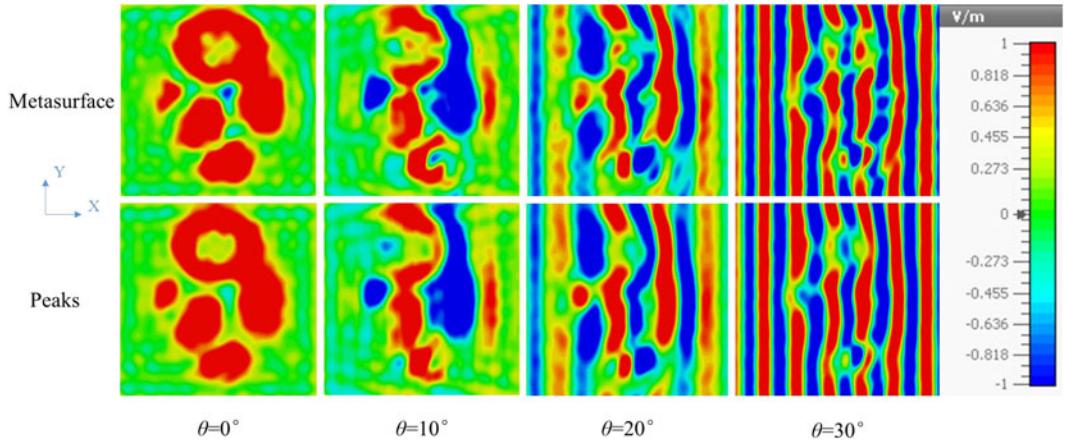

Fig. 4. Interferential electric fields with Y polarization of incident wave and reflective wave at 5.8 GHz in $z = \lambda$ plane. The incident waves for Peaks structure and its corresponding illusion metasurface are the same, which are Y-polarized plane waves with an incident angle θ. The angle θ in the figure is the angle between Z axis and incident direction in XZ plane. Although the metasurface is designed according to the required phase map for normal incidence, the field distributions of illusion metasurface and Peaks structure are similar under the conditions of different incident angles, which means that the proposed illusion metasurface works well in a relative wide incident range.

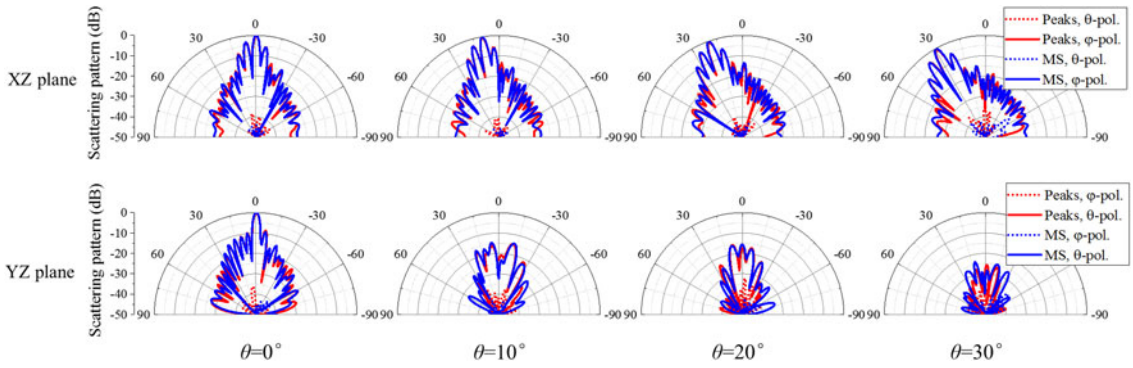

Fig. 5. Normalized scattering patterns at 5.8 GHz corresponding to different incident waves with Y polarization. Although the metasurface is designed according to the required phase map for normal incidence, the scattering patterns of illusion metasurface and Peaks structure are similar under the conditions of different incident angles, which means that the proposed illusion metasurface works well in a relative wide incident range. In the figure, Peaks and MS represent Peaks structure and metasurface, respectively.

orthogonal polarized incident waves. To demonstrate the dual-polarized performance, the normalized scattering patterns at 5.8 GHz corresponding to different incident waves with X polarization are shown in Fig. 6. θ in the Fig. 6 is the angle between Z axis and incident direction in XZ plane, the same as Fig. 5. The scattering patterns of illusion metasurface and Peaks structure are similar under different incident angles, and the main polarized component is more than 35 dB larger than the other component, which indicates that the proposed illusion metasurface has similar performances to orthogonal polarized incident waves.

The proposed planar illusion metasurface is fabricated and measured. A photograph of the metasurface in the measurement configuration is shown in Fig. 3(d) and the schematic diagram of the measurement setup is shown in Fig. 7. The metasurface to be measured is placed on a tray, which can be moved in a 2D plane using three electric step motors with tracks. The minimum step of the step motors is 0.2 mm and the three step motors can be controlled simultaneously with one controller. A probe connected to a soft thin coaxial cable is placed under a horn antenna to measure the interferential field. The thin cable is held by a thin stiff plastic pipe and the pipe holder does

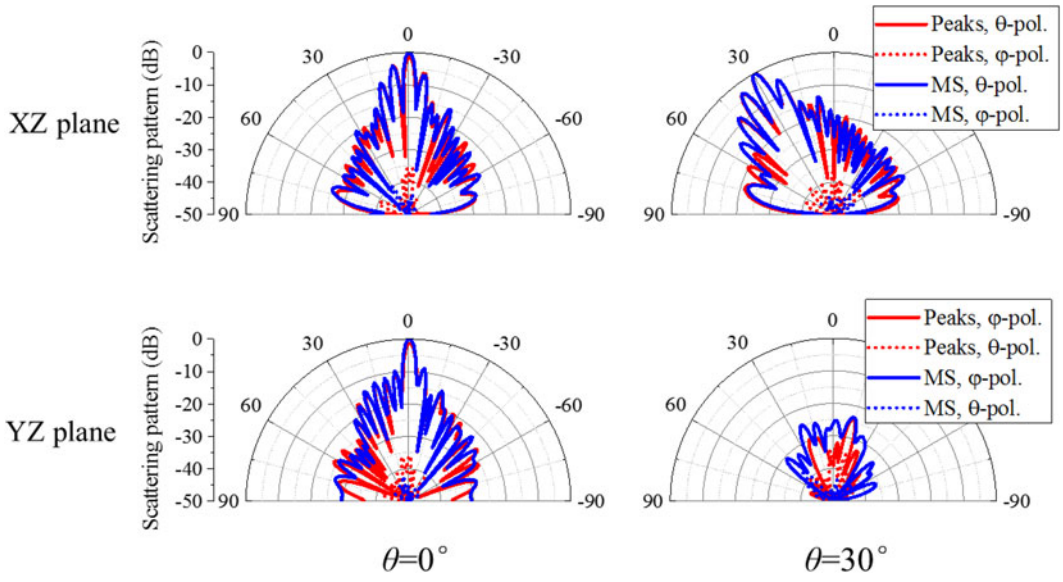

Fig. 6. Normalized scattering patterns at 5.8 GHz corresponding to different incident wave with X polarization. Similar to the case with Y-polarized incident wave, the scattering patterns of illusion metasurface and Peaks structure are similar, which indicates that the proposed metasurface has dual-polarized illusion ability. In the figure, Peaks and MS represent Peaks structure and metasurface, respectively.

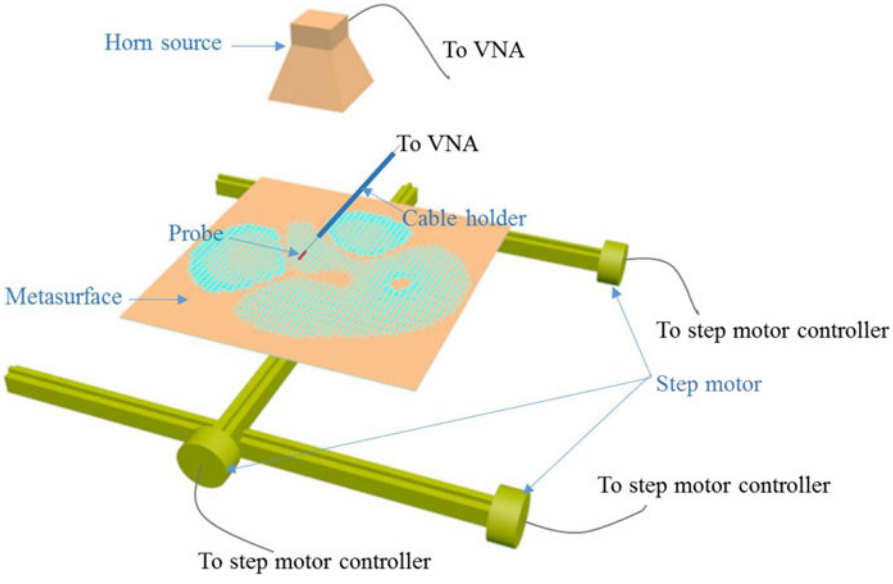

Fig. 7. Schematic diagram of the measurement setup. The metasurface to be measured is placed on a tray, which can be moved in a 2D plane using electric step motors. A probe connected with a soft thin coaxial cable is placed under a horn source to measure the field. The thin cable is held with a thin stiff plastic pipe. The horn and probe are connected to a Vector Network Analyzer (VNA).

not reach the aperture of horn antenna to decrease scattering effect. The probe is arranged right below the center of the horn antenna and the distance between the probe and metasurface is half a wavelength at 5.8 GHz. The horn and probe are connected to an E8361A Vector Network Analyzer (VNA). The positions of the horn and the probe are fixed and the field at different positions above the metasurface can be measured by moving the metasurface.

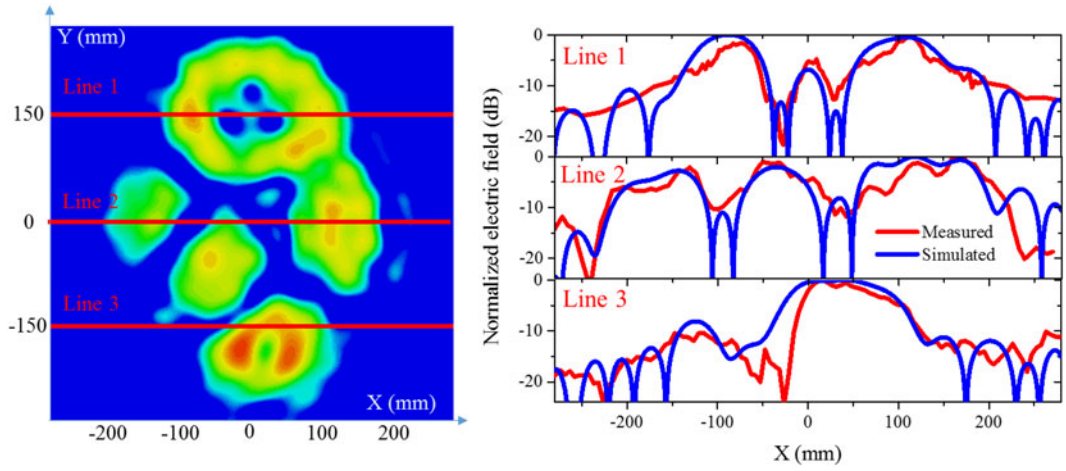

Fig. 8. Simulated and measured amplitudes of interferential electric field in z = λ/2 plane when the proposed illusion metasurface is illuminated with a normal incident wave from horn antenna. In three specific lines, Y = 0 mm and Y = ±150 mm, the measured and simulated electric fields agree well. The difference between simulated and measured results may be mainly caused by the scattering effect of probe and its cable, measurement error, and fabrication error.

The simulated and measured electric field amplitudes of the proposed illusion metasurface illuminated with normal incident wave from horn antenna are shown in Fig. 8. For the measured results, we can see some small fluctuations, which may be caused by the shake of thin probe cable. The difference between simulated and measured results may be mainly caused by the scattering effect of probe and its cable, measurement error, and fabrication error. Although there are a little difference between the measured results and simulated results, their whole variant trends are similar, which indicates that the proposed illusion metasurface works well.

5. Conclusion

This study focuses on creating arbitrary electromagnetic illusions with planar ultrathin metasurfaces. By using dual-polarized subwavelength unit cells, the scattering field of planar metasurfaces can be locally tailored at subwavelength scale and arbitrary scattering field can be rebuilt with the planar metasurfaces. Thus, the scattering field of arbitrary virtual objects can be built by using planar metasurfaces. In other word, we can create arbitrary electromagnetic illusions with planar metasurfaces. Through comparing the scattering fields of Peaks structure and its corresponding illusion metasurfaces, the proposed electromagnetic illusion method is demonstrated numerically and experimentally. Although the proposed illusion metasurface example is designed according to the required phase map for normal incidence, it can still work well in a relative wide incident angle range, which means the proposed method has a strong practicality. It is worth mentioning that the illusion metasurface can have arbitrary shapers to disguise itself as other object and the ultrathin planar metasurface is a good choice for illusion applications as it is very simple and easily-fabricated. In addition, the planar illusion metasurface is the basic unit of other configurations and other forms of metasurface-based illusion devices can be designed based on the similar operation principle. In conclusion, planar ultrathin metasurfaces can be used to create arbitrary electromagnetic illusions.

References

[1] D. Schurig *et al.*, "Metamaterial electromagnetic cloak at microwave frequencies," *Science*, vol. 314, no. 5801, pp. 977–980, 2006.
[2] H. Chen, C. T. Chan, and P. Sheng, "Transformation optics and metamaterials," *Nature Mater.*, vol. 9, no. 5, pp. 387–396, 2010.

[3] H. Chen *et al.*, "Ray-optics cloaking devices for large objects in incoherent natural light," *Nature Commun.*, vol. 4, 2013, Art. no. 3652.
[4] Y. Lai *et al.*, "Illusion optics: The optical transformation of an object into another object," *Phys. Rev. Lett.*, vol. 102, no. 25, 2009, Art. no. 253902.
[5] W. X. Jiang and T. J. Cui, "Radar illusion via metamaterials," *Phys. Rev. E*, vol. 83, no. 2, 2011, Art. no. 026601.
[6] W. X. Jiang, C. W. Qiu, T. Han, S. Zhang, and T. J. Cui, "Creation of ghost illusions using wave dynamics in metamaterials," *Adv. Funct. Mater.*, vol. 23, no. 32, pp. 4028–4034, 2013.
[7] H. X. Xu, G. M. Wang, K. Ma, and T. J. Cui, "Superscatterer illusions without using complementary media," *Adv. Opt. Mater.*, vol. 2, no. 6, pp. 572–580, 2014.
[8] N. Xiang *et al.*, "Bifunctional metasurface for electromagnetic cloaking and illusion," *Appl. Phys. Exp.*, vol. 8, no. 9, 2015, Art. no. 092601.
[9] A. Vitiello *et al.*, "Waveguide characterization of S-band microwave mantle cloaks for dielectric and conducting objects," *Sci. Rep.*, vol. 6, 2016, Art. no. 19716.
[10] Z. H. Jiang and D. H. Werner, "Quasi three dimensional angle tolerant electromagnetic illusion using ultrathin metasurface coatings," *Adv. Funct. Mater.*, vol. 24, no. 48, pp. 7728–7736, 2014.
[11] J. Li and J. B. Pendry, "Hiding under the carpet: A new strategy for cloaking," *Phys. Rev. Lett.*, vol. 101, no. 20, 2008, Art. no. 203901.
[12] R. Liu, C. Ji, J. J. Mock, J. Y. Chin, T. J. Cui, and D. R. Smith, "Broadband ground-plane cloak," *Science*, vol. 323, no. 5912, pp. 366–369, 2009.
[13] H. F. Ma and T. J. Cui, "Three-dimensional broadband ground-plane cloak made of metamaterials," *Nature Commun.*, vol. 1, 2010, Art. no. 21.
[14] L. H. Gabrielli, J. Cardenas, C. B. Poitras, and M. Lipson, "Silicon nanostructure cloak operating at optical frequencies," *Nature Photon.*, vol. 3, no. 8, pp. 461–463, 2009.
[15] T. Ergin, N. Stenger, P. Brenner, J. B. Pendry, and M. Wegener, "Three-dimensional invisibility cloak at optical wavelengths," *Science*, vol. 328, no. 5976, pp. 337–339, 2010.
[16] M. Gharghi *et al.*, "A carpet cloak for visible light," *Nano Lett.*, vol. 11, no. 7, pp. 2825–2828, 2011.
[17] B. Zhang, Y. Luo, X. Liu, and G. Barbastathis, "Macroscopic invisibility cloak for visible light," *Phys. Rev. Lett.*, vol. 106, no. 3, 2011, Art. no. 033901.
[18] C. Faure, O. Richoux, S. Félix, and V. Pagneux, "Experiments on metasurface carpet cloaking for audible acoustics," *Appl. Phys. Lett.*, vol. 108, no. 6, 2016, Art. no. 064103.
[19] Q. Cheng, K. Wu, and G. P. Wang, "All dielectric macroscopic cloaks for hiding objects and creating illusions at visible frequencies," *Opt. Exp.*, vol. 19, no. 23, pp. 23240–23248, 2011.
[20] K. Wu and G. P. Wang, "Hiding objects and creating illusions above a carpet filter using a Fourier optics approach," *Opt. Exp.*, vol. 18, no. 19, pp. 19894–19901, 2010.
[21] Q. Cheng, K. Wu, Y. Shi, H. Wang, and G. P. Wang, "Directionally hiding objects and creating illusions at visible wavelengths by holography," *Sci. Rep.*, vol. 3, 2013, Art. no. 1974.
[22] Q. Cheng, K. Wu, Y. Shi, H. Wang, and G. P. Wang, "Directionally hiding objects and creating illusions above a carpet-like device by reflection holography," *Sci. Rep.*, vol. 5, 2015, Art. no. 8581.
[23] N. Yu *et al.*, "Light propagation with phase discontinuities: Generalized laws of reflection and refraction," *Science*, vol. 334, no. 6054, pp. 333–337, 2011.
[24] S. Sun, Q. He, S. Xiao, Q. Xu, X. Li, and L. Zhou, "Gradient-index meta-surfaces as a bridge linking propagating waves and surface waves," *Nature Mater.*, vol. 11, no. 5, pp. 426–431, 2012.
[25] X. Yin, Z. Ye, J. Rho, Y. Wang, and X. Zhang, "Photonic spin Hall effect at metasurfaces," *Science*, vol. 339, no. 6126, pp. 1405–1407, 2013.
[26] D. Lin, P. Fan, E. Hasman, and M. L. Brongersma, "Dielectric gradient metasurface optical elements," *Science*, vol. 345, no. 6194, pp. 298–302, 2014.
[27] R. Wang, B.-Z. Wang, Z.-S. Gong, and X. Ding, "Far-field subwavelength imaging with near-field resonant metalens scanning at microwave frequencies," *Sci. Rep.*, vol. 5, 2015, Art. no. 11131.
[28] N. Yu and F. Capasso, "Flat optics with designer metasurfaces," *Nature Mater.*, vol. 13, no. 2, pp. 139–150, 2014.
[29] N. M. Estakhri and A. Alù, "Ultra-thin unidirectional carpet cloak and wavefront reconstruction with graded metasurfaces," *IEEE Antennas Wireless Propag. Lett.*, vol. 13, pp. 1775–1778, 2014.
[30] Y. Yang *et al.*, "Full polarization 3D metasurface cloak with preserved amplitude and phase," *Adv. Mater.*, vol. 28, no. 32, pp. 6866–6871, 2016.
[31] B. Orazbayev, N. M. Estakhri, A. Alù, and M. Beruete, "Experimental demonstration of metasurface based ultrathin carpet cloaks for millimeter waves," *Adv. Opt. Mater.*, vol. 5, no. 1, 2017, Art. no. 1600606.
[32] L. Y. Hsu, T. Lepetit, and B. Kante, "Extremely thin dielectric metasurface for carpet cloaking," *Prog. Electromagn. Res.*, vol. 152, pp. 33–40, 2015.
[33] X. Ni, Z. J. Wong, M. Mrejen, Y. Wang, and X. Zhang, "An ultrathin invisibility skin cloak for visible light," *Science*, vol. 349, no. 6254, pp. 1310–1314, 2015.
[34] H. Esfahlani, K. Sami, H. Lissek, and J. R. Mosig, "Acoustic carpet cloak based on an ultrathin metasurface," *Phys. Rev. B*, vol. 94, no. 1, 2016, Art. no. 014302.
[35] M. Dubois, C. Shi, Y. Wang, and X. Zhang, "A thin and conformal metasurface for illusion acoustics of rapidly changing profiles," *Appl. Phys. Lett.*, vol. 110, no. 15, 2017, Art. no. 151902.